

SYNTHESIS, CHARACTERIZATION, AND COMPUTATIONAL STUDIES OF *N*-(9E)-8,10,17- TRIAZATETRACYCLO[8.7.0.0^{2,7}.0^{11,16}]HEPTADECA- 1(17),2,4,6,11(16),12,14-HEPTAEN-9-YLIDENE]BENZAMIDE*

F. Odame^{1,2**}, E. C. Hosten², and Z. R. Tshentu²

N-(9E)-8,10,17-Triazatetracyclo[8.7.0.0^{2,7}.0^{11,16}]heptadeca-1(17),2,4,6,11(16),12,14-heptaen-9-ylidene]benzamide (**I**) is synthesized and characterized by spectroscopy, microanalysis, and single crystal X-ray diffractometry. Compound **I** crystallizes in the monoclinic space group *P*2₁/c with *a* = 15.8980(7) Å, *b* = 4.8067(2) Å, *c* = 21.0455(10) Å, β = 101.153(2)°, and *Z* = 4. The experimental bond lengths and bond angles are contrasted with computed bond lengths and bond angles.

DOI: 10.1134/S0022476620080016

Keywords: triazatetracyclic, benzoyl isothiocyanate, benzoyl chloride.

INTRODUCTION

Triazatetracyclics have been obtained by various methods [1-5]. Two protocols have been developed for the synthesis of amino-functionalized benzo[4,5]imidazo[2,1-a]isoquinolines and isoquinolino[3,4-b]quinoxalines from *o*-phenylene diamines and *o*-cyanobenzaldehydes [6]. An efficient tandem route to the synthesis of iodoisoquinoline-fused benzimidazole derivatives, including an iodocyclization strategy, has been developed. A variety of 2-ethynylbenzaldehydes underwent the tandem reaction with benzenediamines and iodine to afford respective iodoisoquinoline-fused benzimidazoles [7]. An efficient and facile Au(I)/Ag(I) cascade method has been developed for the one-pot synthesis of complex polycyclic heterocycles of benzo[4,5]imidazo[1,2-c]pyrrolo[1,2-a]quinazzoline derivatives through treatment of substituted 2-(1H-benzo[d]imidazole-2-yl)anilines with 4-pentyneoic or 5-hexynoic acids [8]. Most HIV-1 protease inhibitors are designed to fit the active site of the enzyme [9]. This allows the HIV-1 protease inhibitors to compete with the natural substrate. A class of antimalarial pyrido[1,2-a]benzimidazoles has been synthesized and evaluated for the antiplasmodial activity and cytotoxicity [10]. Imidazoyl-*o*-nitrobenzamides and isothiocyanates have been reacted in the presence of zinc and TiCl₄ in THF, with an *in situ* reduction of the nitro group occurring before cyclization [11]. Substituted methyl anthranilates have been reacted with various iso(thio)cyanates in DMSO/H₂O using microwave irradiation to generate diverse 2,4(1H,3H)-quinazolinediones or 2-thioxoquinazolinones [12].

¹Department of Basic Sciences, University of Health and Allied Sciences, Ho, P. R. Ghana; **felixessah15@gmail.com.

²Department of Chemistry, Nelson Mandela University, Port Elizabeth, South African Republic. Original article submitted December 16, 2019; revised January 31, 2020; accepted February 3, 2020.

* Supplementary materials are available for this article at doi 10.1134/S0022476620080016 and are accessible for authorized users.

In this work, *N*-[(9E)-8,10,17-triazatetracyclo[8.7.0.0^{2,7}.0^{11,16}]heptadeca-1(17),2,4,6,11(16),12,14-heptaen-9-ylidene]benzamide has been synthesized and characterized with IR, NMR, GC-MS, and elemental analysis. The single crystal X-ray structure has been discussed; the experimental bond lengths and bond angles were compared to the computed ones. The HOMO and LUMO energy levels were discussed, too.

EXPERIMENTAL

Materials and methods. Analytical grade reagents and solvents for the synthesis such as 2-(2'-aminophenyl)-1*H*-benzimidazole and benzoyl chloride were obtained from Sigma Aldrich (USA) whilst acetone and ammonium thiocyanate were obtained from Merck Chemicals (SA). The chemicals were used as received (i.e. without further purification). ¹H and ¹³C NMR spectra were recorded on a Bruker Avance AV 400 MHz spectrometer operating at 400 MHz for ¹H and 100 MHz for ¹³C using dimethyl sulfoxide as the solvent and tetramethylsilane as the internal standard. Chemical shifts are expressed in ppm. FTIR spectra were recorded on a Bruker Platinum ATR Spectrophotometer Tensor 27. Elemental analyses were performed using Vario Elementar Microcube ELIII. Melting points were obtained using a Stuart Lasec SMP30 and were reported uncorrected whilst the masses were determined using an Agilent 7890A GC system connected to 5975C VL-MSC with electron impact as the ionization mode and detection by a triple-axis detector. The GC system was fitted with a 30 m×0.25 mm×0.25 μm DB-5 capillary column. Helium was used as carrier gas at a flow rate of 1.63 mL/min with an average velocity of 30.16 cm/s and a pressure of 63.73 kPa.

***N*-(9E)-8,10,17-triazatetracyclo[8.7.0.0^{2,7}.0^{11,16}]heptadeca-1(17),2,4,6,11(16),12,14-heptaen-9-ylidene]benzamide (I).** Ammonium thiocyanate (0.02 mol, 1.5224 g) was dissolved in 40 mL of acetone. The respective benzoyl chloride derivative (0.02 mol) was added, followed by heating under reflux at 100–120 °C for 2 h. The benzoyl isothiocyanate derivative (0.02 mol) obtained was filtered and 2-(2-aminophenyl)-1*H*-benzimidazole (0.02 mol, 4.185 g) was added to the filtrate and refluxed at 100–120 °C for 6 h. The product obtained was filtered and recrystallized from DMSO:toluene (1:1) as a yellow solid. Melting point = 205–206 °C. Yield = 78.27%. ¹H NMR (ppm): 13.26 (br, 1H, N–H), 8.36 (m, 6H), 8.01 (d, 1H, *J* = 8.0 Hz), 7.77 (d, 1H, *J* = 8.0 Hz), 7.50 (t, 1H, *J* = 8.0 Hz), 7.35 (t, 1H, *J* = 7.2, 7.6 Hz). ¹³C NMR (ppm): 149.7 (C), 129.8 (C–H), 126.4 (C–H), 124.0 (C–H), 123.6 (C–H), 121.9 (C–H). IR (ν_{max} , cm^{−1}): 3056 (N–H), 1786 (C=O), 1633, 1593 (C=C), 1565 (C=C), 1547, 1479. LRMS (*m/z*, M⁺): Found for C₂₁H₁₄N₄O 338.28; Expected mass 338.36; Anal. calcd for C₂₁H₁₄N₄O (%): C 74.54, H 4.17, N 16.56. Found for C₂₁H₁₄N₄O (%): C 74.62, H 4.26, N 16.70.

X-ray crystallography. The X-ray diffraction analysis of **I** was performed at 200 K using a Bruker KAPPA APEX II diffractometer with monochromated MoK_α radiation (λ = 0.71073 Å). APEX II [13] was used for the data collection, the cell refinement, and the data reduction. The structures were solved by direct methods using SHELXS-2013 [13] and refined by least-squares procedures using SHELXL-2013 [14] with SHELXLE [13] as a graphical interface. All non-hydrogen atoms were refined anisotropically. Carbon-bound H atoms were placed in calculated positions (C–H 0.95 Å for aromatic carbon atoms and C–H 0.99 Å for methylene groups) and were included in the refinement in the riding model approximation with U_{iso} (H) set to 1.2 U_{eq} (C). The H atoms of methyl groups were allowed to rotate with a fixed angle around the C–C bond to best fit the experimental electron density (HFIX 137 in the SHELX program suite [14]) with U_{iso} (H) set to 1.5 U_{eq} (C). Nitrogen-bound H atoms were located on a difference Fourier map and refined freely. Data were corrected for absorption effects, using the numerical method implemented in SADABS [15].

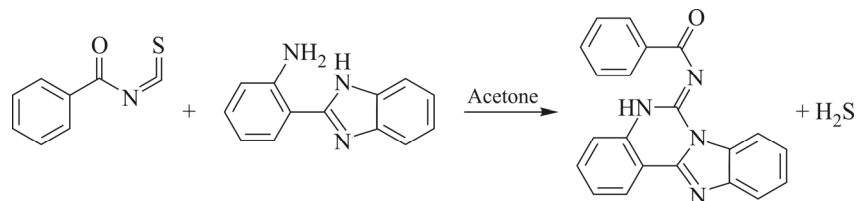
COMPUTATIONAL STUDIES

The calculations were carried out using the Gaussian 09 program [16]. Molecular geometries of the singlet ground state of all the compounds were fully optimized in the gas phase at the density functional theory (DFT) level of theory using hybrid B3LYP [17–19], B3PW91, and wB97XD functionals together with the 6-31G(*d,p*) basis set. For compound **I** a frequency calculation was carried out to ensure that the optimized molecular structure corresponded to a minimum [20],

thus only positive frequencies were expected. The HOMO and LUMO results as well as the information for bond lengths and bond angles were obtained using the Avogadro method.

RESULTS AND DISCUSSION

Characterization of *N*-(9E)-8,10,17-triazatetracyclo[8.7.0.0^{2,7}.0^{11,16}]heptadeca-1(17),2,4,6,11(16),12,14-heptaen-9-ylidene]benzamide (Scheme 1). The IR spectrum showed a signal at 3056 cm⁻¹ for the N–H stretch. A signal was observed at 1633 cm⁻¹ for the C=O stretch. The C–N stretch was observed near 1593 cm⁻¹. The ¹H NMR spectrum showed signals at 14.38 ppm for the NH proton. Aromatic protons were observed between 8.36 ppm and 6.92 ppm. The ¹³C NMR spectra showed signals between 144.4 ppm and 104.4 ppm for aromatic carbon atoms.



Scheme 1. Synthesis of *N*-(9E)-8,10,17-triazatetracyclo[8.7.0.0^{2,7}.0^{11,16}]heptadeca-1(17),2,4,6,11(16),12,14-heptaen-9-ylidene].

The triazatetracyclic acetyl derivative has been reported [21] to be synthesized by the reaction of acetyl chloride with ammonium thiocyanate to give acetyl thiocyanate which was then refluxed with 2-(2-aminophenyl)-1H-benzimidazole for 6 h to give *N*-(9E)-8,10,17-triazatetracyclo[8.7.0.0^{2,7}.0^{11,18}]heptadeca-1(17),2(7),3,5,11,13,15-heptaen-9-ylidene] acetamide (methyl derivative). The reaction was reported to proceed as the attack of the thiocyanate carbon atom by the lone pair from the nitrogen atom of the 2-aminophenyl group. A shift of the electron density on the carbonyl group onto the oxygen atom was proposed to allow the cleavage of C=N bond, forming another C=N bond with the carbonyl group. A subsequent attack by the lone pair of the nitrogen atom led to the formation of thiol and alcohol. A rearrangement was reported to occur followed by the loss of hydrogen sulphide (which turns lead acetate paper black), leading to the formation of the final product. The reaction for the phenyl derivative being reported here proceeds by the same mechanism as for the triazatetracyclic acetyl derivative [21]. Two triazaspiro tetracycles have been synthesized by the reaction of 2-(2'-aminophenyl)-1H-benzimidazole and 4-methylcyclohexanone or 3-methylcyclohexanone under reflux and solvent free conditions [22]. In this reaction, the triazatetracyclic backbone was obtained by the attachment of cyclic ketone and the subsequent loss of water whilst the formation of the triazatetracyclic acetyl and phenyl derivatives proceeded through the isothiocyanate intermediate with the formation of thione and the subsequent loss of hydrogen sulphide.

Crystal structure determination. The crystallographic data, selected experimental and computed bond lengths and bond angles for compound **I** are provided in Tables 1 and 2. Compound **I** crystallized in the monoclinic space group *P*2₁/c with *a* = 15.8980(7) Å, *b* = 4.8067(2) Å, *c* = 21.0455(10) Å, β = 101.153(2)°, and *Z* = 4. Compound **I** undergoes the hydrogen bonding between N3---H3 and O1 and also between C13---H13 and N4. The triazaacetyl derivative crystallized in the monoclinic space group *P*2₁/n with *a* = 17.5552(17) Å, *b* = 4.6163(4) Å, *c* = 17.7662(17) Å, β = 115.953(3)°, and *Z* = 4 [21], whilst the 4-methyl triazaspiro tetracycle derivative also crystallized in the monoclinic space group *P*2₁/n with *a* = 12.9495(4) Å, *b* = 16.2186(4) Å, *c* = 15.6429(3) Å, β = 91.857(1)°, α = γ = 90°, *Z* = 8 [22]. The triazaacetyl and triazabenzyol derivatives are almost planar. The ORTEP diagram of compound **I** is presented in Fig. 1. The bond distance O1–C3 = 1.245(1) Å in compound **I** is consistent with the carbonyl C=O bond, whilst the N1–C1 and N2–C1 bond distances were 1301(2) Å and 1.406(2) Å respectively.

TABLE 1. Crystallographic Data and Structure Refinement Summary for Compound **I**

| Parameter | Compound I |
|---|--|
| Formula | C ₂₁ H ₁₄ N ₄ O |
| CCDC number | 1448792 |
| Formula weight | 338.36 |
| Crystal system | Monoclinic |
| Space group | P2 ₁ /c |
| <i>a</i> , <i>b</i> , <i>c</i> , Å | 15.8980(7), 4.8067(2), 21.0455(10) |
| β, deg | 101.153(2) |
| <i>V</i> , Å ³ | 1577.86(12) |
| <i>Z</i> | 4 |
| <i>D</i> _{calc} , g/cm ³ | 1.424 |
| μ(MoK _α), mm | 0.092 |
| <i>F</i> (000) | 704 |
| Crystal size, mm | 0.05×0.32×0.59 |
| Temperature, K | 200 |
| Radiation, Å | 0.71073 |
| θ _{min-max} , deg | 2.0-28.3 |
| Dataset | -21:21; -6:6; -27:28 |
| Tot., Uniq. Data, <i>R</i> (int) | 21774, 3928, 0.022 |
| Observed data (<i>I</i> >2.0σ(<i>I</i>)) | 3165 |
| <i>N</i> _{ref} / <i>N</i> _{par} | 3928 / 239 |
| <i>R</i> / <i>wR</i> ₂ | 0.0375 / 0.1047 |
| <i>S</i> | 1.03 |
| Max. and Av. Shift / Error | 0.00 / 0.00 |
| Min. / Max. Resd. Dens., e/Å ³ | -0.20 / 0.27 |

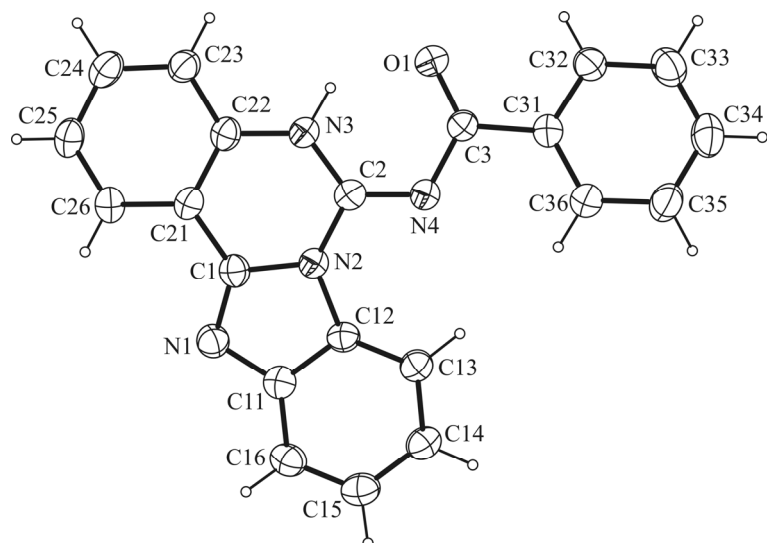
**Fig. 1.** ORTEP view of *N*-(9E)-8,10,17-triazatetracyclo[8.7.0.0^{2,7}.0^{11,16}]heptadeca-1(17),2,4,6,11(16),12,14-heptaen-9-ylidene]benzamide (**I**) with 50% probability displacement ellipsoids and atom labeling.

TABLE 2. Summary of Experimental and Theoretical Bond Lengths and Bond Angles for Compound **I** Obtained by B3LYP, CAM-B3LYP, B3PW91, WB97XD, and M06 functionals and the 6-31G(*d,p*) Basis Set

| Experimental | B3LYP | CAM-B3LYP | B3PW91 | WB97XD | M06 | Min. deviation | Max. deviation | |
|-----------------|----------|-----------|--------|--------|-------|----------------|----------------|-------|
| Bond length, Å | | | | | | | | |
| O1–C3 | 1.245(1) | 1.229 | 1.222 | 1.227 | 1.221 | 1.222 | 0.016 | 0.024 |
| N1–C1 | 1.301(2) | 1.303 | 1.293 | 1.301 | 1.295 | 1.297 | 0.002 | 0.006 |
| N1–C11 | 1.406(1) | 1.387 | 1.387 | 1.383 | 1.388 | 1.383 | 0.019 | 0.023 |
| N2–C1 | 1.406(1) | 1.422 | 1.411 | 1.415 | 1.408 | 1.414 | 0.002 | 0.016 |
| N2–C2 | 1.378(1) | 1.392 | 1.386 | 1.388 | 1.387 | 1.387 | 0.008 | 0.014 |
| N2–C12 | 1.405(1) | 1.408 | 1.405 | 1.402 | 1.402 | 1.404 | 0.001 | 0.003 |
| N3–C2 | 1.345(2) | 1.374 | 1.367 | 1.370 | 1.368 | 1.370 | 0.022 | 0.029 |
| N3–C22 | 1.394(1) | 1.391 | 1.390 | 1.386 | 1.391 | 1.388 | 0.003 | 0.006 |
| N4–C2 | 1.317(1) | 1.294 | 1.288 | 1.292 | 1.288 | 1.287 | 0.023 | 0.03 |
| N4–C3 | 1.368(1) | 1.383 | 1.378 | 1.379 | 1.381 | 1.380 | 0.01 | 0.015 |
| Bond angle, deg | | | | | | | | |
| C1–N1–C11 | 104.8(1) | 105.5 | 105.4 | 105.3 | 105.1 | 105.2 | 0.3 | 0.7 |
| C1–N2–C2 | 124.1(1) | 123.3 | 123.3 | 123.4 | 123.6 | 123.6 | 0.5 | 0.8 |
| C1–N2–C12 | 105.9(1) | 105.5 | 105.4 | 105.4 | 105.6 | 105.4 | 0.3 | 0.5 |
| C2–N2–C12 | 130.0(1) | 131.2 | 131.2 | 131.0 | 130.8 | 131.0 | 0.8 | 1.2 |
| N3–C22–C23 | 120.0(1) | 121.2 | 121.2 | 121.3 | 121.1 | 121.2 | 1.1 | 1.3 |
| C2–N3–C22 | 125.4(1) | 127.0 | 126.7 | 127.0 | 126.3 | 126.8 | 0.9 | 1.6 |
| C2–N4–C3 | 118.6(1) | 125.4 | 124.6 | 125.2 | 124.1 | 124.9 | 5.5 | 6.8 |
| N1–C1–N2 | 113.3(1) | 113.1 | 113.4 | 113.2 | 113.5 | 113.4 | 0.1 | 0.2 |
| N1–C1–C21 | 128.6(1) | 127.7 | 127.6 | 127.7 | 127.7 | 127.7 | 0.9 | 1.0 |
| N2–C1–C21 | 118.1(1) | 119.1 | 118.9 | 119.0 | 118.7 | 118.8 | 0.6 | 1.0 |
| N2–C2–N3 | 115.4(1) | 113.8 | 114.0 | 113.9 | 114.0 | 113.8 | 1.4 | 1.6 |
| N2–C2–N4 | 118.4(1) | 128.8 | 128.4 | 128.7 | 127.9 | 128.3 | 9.5 | 10.4 |
| N3–C2–N4 | 126.2(1) | 117.3 | 117.5 | 117.4 | 118.0 | 117.9 | 8.2 | 8.9 |
| O1–C3–N4 | 126.2(1) | 123.9 | 123.8 | 124.0 | 123.7 | 123.9 | 2.2 | 2.5 |
| O1–C3–C31 | 119.1(1) | 121.5 | 121.4 | 121.5 | 121.6 | 121.7 | 2.3 | 2.6 |

The N2–C2–N3 bond angle of 115.4(12)° confirms the sp^2 hybridization of the C2 carbon atom, whilst the C1–N1–C11 bond angle is 104.8(1)°. The C22–N3–C2–N4 torsion angle of 179.9(2)° confirms the planarity around C2. The C12–N2–C2–N4 and C22–N3–C2–N2 torsion angles of 0.2(2)° and 0.4(2)° respectively also confirmed that C2 was planar (Table S1). The bond lengths for the six-member ring C22–C21–C1–N2–C2–N3 ranged from 1.345 Å to 1.406 Å, confirming that the bonds are neither distinctly single bonds (1.32 Å) nor distinctly double bonds (1.47 Å). This suggest that there is electron delocalization over the entire ring to achieve the stability, and hence, the planarity of the ring. Fig. 1 gives the ORTEP view of compound **I** with 50% probability displacement ellipsoids and atom labeling.

The O1–C3 bond length was experimentally determined as 1.245° whilst the computed bond length gave deviations of 0.016 Å to 0.024 Å from the experimental values. For the N1–C1, N1–C11, N2–C1, and N2–C2 amide bonds the experimental bond lengths obtained were 1.301(2) Å, 1.406(1) Å, 1.406(1) Å, and 1.378(1) Å, respectively; the computed values deviated by 0.002 Å and 0.023 from the experimental values. The C1–N2–C2, C1–N2–C12, N1–C1–N2 bond angles were experimentally determined as 124.1(1)°, 105.9(1)°, and 113.3(1)° whilst the computed values gave deviations between 0.2° and 0.8°, representing the lowest deviations from the computed values. The C2–N4–C3, N2–C2–N4, and N3–C2–N4 bond angles were obtained from the experiment as 118.6(1)°, 118.4(1)°, and 126.2(1)°, respectively, whilst the computed values gave deviations between 6.8° and 10.4°. The large deviations that only occurred in these angles might be due to the

fact that gas phase considerations in computations are different from the measurement obtained from the single crystal structure. Fig. 2 shows the packing of the compounds in the unit cell of compound **I**. Four compounds are packed in the unit. There is an intramolecular hydrogen bond between the carbonyl oxygen atom and the amide hydrogen atom.

Fig. 3 gives the intermolecular interactions that exists between the molecules of compound **I**. There are intermolecular interactions between the hydroxyl group of one molecule and the electron density of nearest π -system of a benzene ring of the adjacent molecule, inducing a dipole due to the polar character of the hydroxyl group. Van der Waals interactions also occur between the electron clouds of the adjacent π -systems. A network of these interactions exists throughout the compound and is responsible for the high melting point of compound **I**.

There exists a marked difference in the arrangement of molecules within the crystal lattice of the triazaacetyl derivative compared to that in the triazobenzoyl derivative. The difference consists in that some molecules are stacked together and held by Van der Waals forces. This is only possible because of the absence of a benzoyl moiety in the triazaacetyl derivative molecules. Fig. 4 gives the stacking of the molecules within the crystal lattice of the triazaacetyl derivative [21].

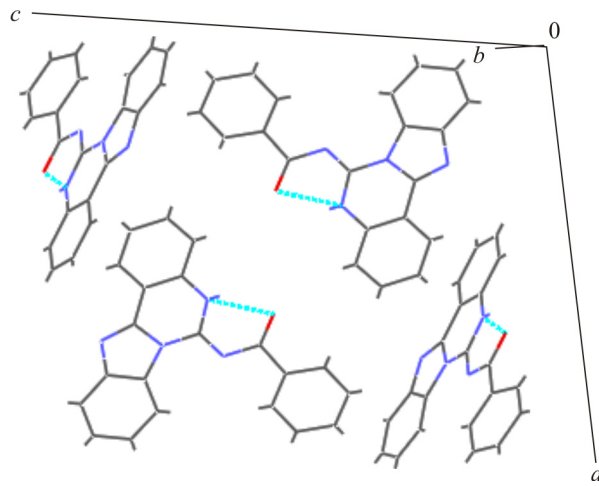


Fig. 2. Packing of the unit cell of compound **I**.

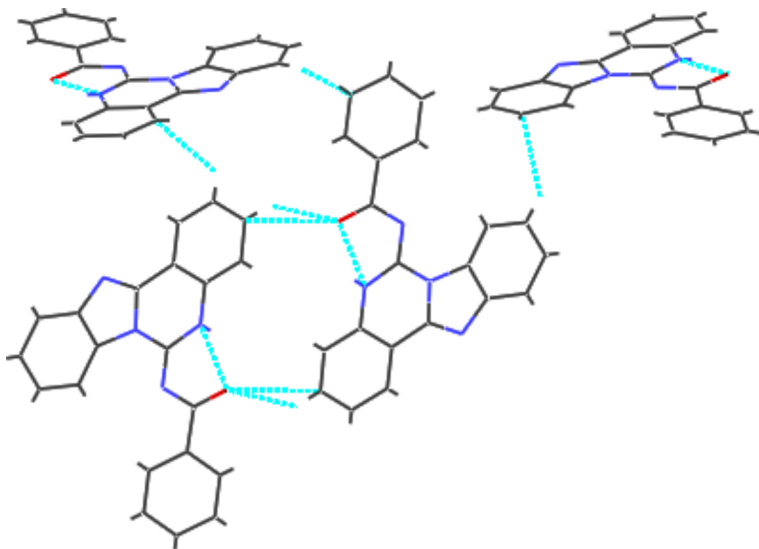


Fig. 3. Intermolecular interactions in compound **I**.

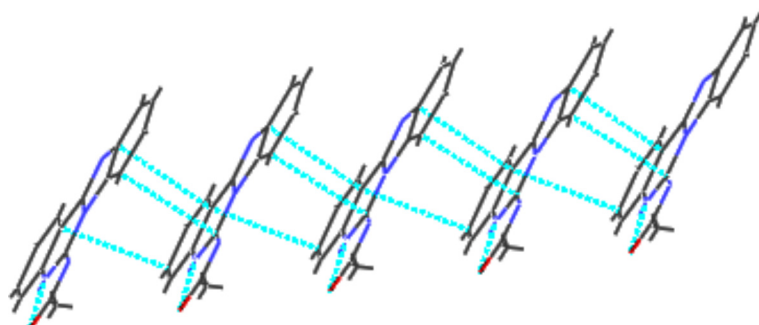


Fig. 4. Stacking of molecules of the triazaacetyl derivative within the crystal lattice [21].

Fig. 5 illustrates the intermolecular interactions in the triazaacetyl derivative. In addition to the stacking which occurs between its molecules there is also a sideways interaction among the adjacent molecules, which involves the hydroxyl moiety and the methyl group of one molecule and the π -system from the adjacent molecule.

Fig. 6 gives the packing in the unit cell of the 4-methyl triazaspiro tetracycle derivative. The unit cell contains 8 molecules in contrast to the 4 molecules found in the unit cells of both the triazaacetyl tetracyclic and triazabenzoyl tetracyclic derivative.

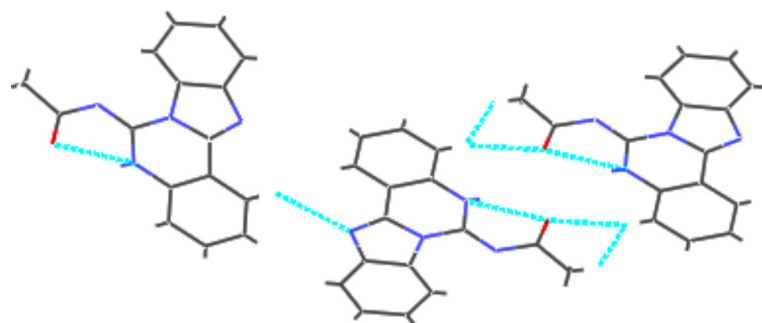


Fig. 5. Intermolecular interactions in the triazaacetyl derivative [21].

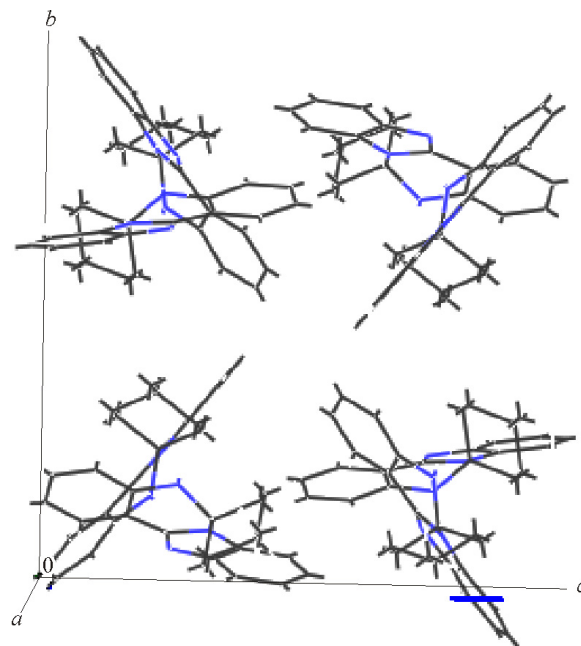


Fig. 6. Packing in the unit cell of the 4-methyl triazaspiro tetracycle derivative [22].

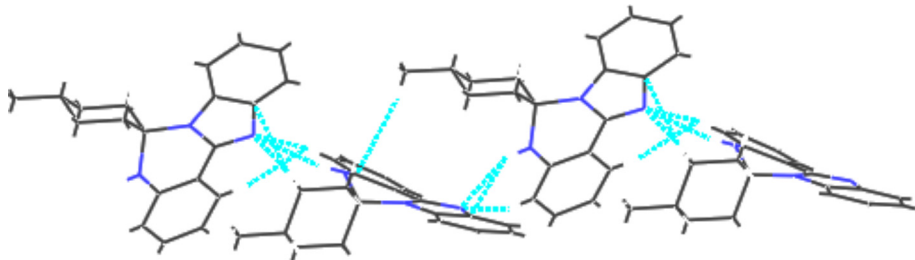


Fig. 7. Intermolecular interactions in the methyl triazaspiro tetracycle derivative [22].

TABLE 3. HOMO–LUMO Energy Levels of *N*-[(Benzyl)Methanethioyl]Benzamide Compound **I** Calculated by B3LYP, CAM-B3LYP, B3PW91, WB97XD, and M06 Functionals and the 6-31G(*d,p*) Basis Set

| HOMO–LUMO | B3LYP | CAM-B3LYP | B3PW91 | WB97XD | M06 |
|-------------------|----------|-----------|----------|----------|----------|
| LUMO+4 | 0.00160 | 0.05213 | −0.00171 | 0.07092 | 0.00637 |
| LUMO+3 | −0.00516 | 0.04569 | −0.00833 | 0.06585 | 0.00068 |
| LUMO+2 | −0.02182 | 0.02758 | −0.02546 | 0.04670 | −0.01649 |
| LUMO+1 | −0.05145 | −0.00501 | −0.05512 | 0.01478 | −0.04485 |
| LUMO | −0.06025 | −0.01484 | −0.06389 | 0.00561 | −0.05440 |
| HOMO | −0.21639 | −0.26505 | −0.22081 | −0.28666 | −0.22805 |
| HOMO−1 | −0.23405 | −0.28770 | −0.23803 | −0.30982 | −0.24740 |
| HOMO−2 | −0.23980 | −0.29225 | −0.24432 | −0.31404 | −0.25251 |
| HOMO−3 | −0.24267 | −0.30114 | −0.24677 | −0.32378 | −0.25774 |
| HOMO−4 | −0.24777 | −0.30219 | −0.25253 | −0.32515 | −0.26013 |
| HOMO–LUMO gap, eV | 0.15614 | 0.25021 | 0.15692 | 0.29227 | 0.17365 |

Fig. 7 illustrates intermolecular interactions in the 4-methyl triazaspiro tetracycle derivative. There are no intramolecular interactions in a 4-methyl triazaspiro molecule, however, there exist intermolecular interactions between a nitrogen atom and the 4-methyl cyclohexanyl moiety of the adjacent molecule or its nitrogen atom [22].

Table 3 gives the HOMO–LUMO energy levels of compounds **I** calculated by B3LYP, CAM-B3LYP, 3PW91, WB97XD, and M06 functionals and the 6-31G(*d,p*) basis set. The HOMO and LUMO gave energy gaps are between 0.15614 eV and 0.29227 eV. The high energy gap is consistent with the high melting point of the compound and its low solubility in most solvents.

CONCLUSIONS

N-(9E)-8,10,17-Triazatetracyclo[8.7.0^{2,7}.0^{11,16}]heptadeca-1(17),2,4,6,11(16),12,14-heptaen-9-ylidene]benzamide has been synthesized from the reaction of benzoyl isothiocyanate with 2(2-aminophenyl)-1*H*-benzimidazole. The compound was characterized with spectroscopy, microanalysis, and GC-MS. The single crystal XRD molecular structure of *N*-(9E)-8,10,17-triazatetracyclo[8.7.0^{2,7}.0^{11,16}]heptadeca-1(17),2,4,6,11(16),12,14-heptaen-9-ylidene] benzamide was discussed. The experimental bond lengths and bond angles have been compared to the computed ones. The HOMO and LUMO energy levels were also discussed.

ACKNOWLEDGMENTS

The authors would like to thank MRC for the financial support. F. Odame would like to thank NRF for the financial support.

CONFLICT OF INTERESTS

The authors declare that they have no conflict of interests.

REFERENCES

1. T. M. Das, C. P. Rao, and E. Kolehmainen. *Carbohydr. Res.*, **2001**, *334*, 261–269.
2. Y. S. Chhonker, B. Veenu, S. R. Hasim, N. Kaushik, D. Kumar, and P. Kumar. *Eur. J. Adv. Chem. Res.*, **2009**, *6*(S1), S342–S346.
3. H. Pessoa-Mahana, C. D. Pessoa-Mahana, R. Salazar, J. A. Valderrama, E. Saez, and R. Araya-Maturana. *Synthesis*, **2004**, *3*, 436–440.
4. P. P. Joshi and S. G. Shirodkar. *World J. Pharm. Pharm. Sci.*, **2014**, *3*(9), 950–958.
5. B. A. Insuasty, H. Torres, J. Quiroga, R. Abonia, R. Rodriguez, M. Nogeras, A. Sanchez, C. Saitz, S. L. Avarez, and S. A. Zacchino. *J. Chil. Chem. Soc.*, **2006**, *51*(2), 927–932.
6. A. L. Bagdasarian, H. H. Nguyen, T. A. Palazzo, J. C. Fettinger, M. J. Haddadin, and M. J. Kurth. *J. Org. Chem.*, **2016**, *81*, 3924–3928.
7. H. C. Ouyang, R. Y. Tang, P. Zhong, X. G. Zhang, and J. H. Li. *J. Org. Chem.*, **2011**, *76*, 223–228.
8. X. Ji, Y. Zhou, J. Wang, H. Zhao, H. Jiang, and H. Liu. *J. Org. Chem.*, **2013**, *78*, 4312–4318.
9. A. J. Ndakala, R. K. Gessner, P. W. Gitari, N. October, K. L. White, A. Hudson, F. Fakorede, D. M. Shackleford, M. Kaiser, C. Yeates, S. A. Charman, and K. Chibale. *J. Med. Chem.*, **2011**, *54*, 4581–4589.
10. I. T. Weber and J. Agniswamy. *Viruses*, **2009**, *1*, 1110–1136.
11. G. Dou, M. Wang, and D. Shi. *J. Comb. Chem.*, **2009**, *11*, 151–154.
12. Z. Li, H. Huang, H. Sun, H. Jiang, and H. Liu. *J. Comb. Chem.*, **2008**, *10*, 484–486.
13. APEX2, SADABS and SAINT. Madison, Bruker AXS: WI, USA, **2010**.
14. G. M. Sheldrick. *Acta Crystallogr., Sect. A*, **2008**, *64*, 112–122.
15. C. B. Hübschle, G. M. Sheldrick, and B. Dittrich. *J. Appl. Crystallogr.*, **2011**, *44*, 1281–1284.
16. M. J. Frisch, G. W. Trucks, H. B. Schlegel, G. E. Scuseria, M. A. Robb, J. R. Cheeseman, J. A. Montgomery, T. Vreven, K. N. Kadin, J. C. Burant, J. M. Millam, S. S. Iyengar, J. Tomasi, V. Barone, B. Mennucci, M. Cossi, G. Scalmani, N. Rega, G. A. Petersson, H. Nakatsuji, M. Hada, M. Hears, K. Toyota, R. Fukuda, J. Hasegawa, M. Ishida, T. Nakajima, Y. Honda, O. Kitao, H. Nakai, M. Klene, X. Li, J. E. Knox, H. P. Hratchian, J. B. Cross, V. Bakken, C. Adamo, J. Jaramillo, R. Gomperts, R. E. Stratmann, O. Yazyev, A. J. Austin, R. Cammi, C. Pomelli, J. W. Ochterski, P. Y. Ayala, K. Morokuma, G. A. Voth, P. Salvador, J. J. Dannenberg, V. G. Zakrzewski, S. Dapprich, A. D. Daniels, M. C. Strain, O. Farkas, D. K. Malick, A. D. Rabuck, K. Raghavachari, J. B. Foresman, J. V. Ortiz, Q. Cui, A. G. Baboul, S. Clifford, J. Cioslowski, B. B. Stefanov, G. Liu, A. Liashenko, P. Piskorz, I. Komaromi, R. L. Martin, D. J. Fox, T. Keith, M. A. Al-Laham, C. Y. Peng, A. Nanayakkara, M. Challacombe, P. M. W. Gill, B. Johnson, W. Chen, M. W. Wong, C. Gonzalez, J. A. Pople. Gaussian 03, revision B03. Gaussian: Pittsburgh, **2003**.
17. P. C. Hariharan and J. A. Pople. *Theor. Chim. Acta*, **1973**, *28*, 213–322.
18. P. C. Hariharan and J. A. Pople. *Mol. Phys.*, **1974**, *27*, 209–214.
19. W. Kohn, A. D. Becke, and R. G. Parr. *J. Phys. Chem.*, **1996**, *100*, 12974–12980.
20. A. Frisch, A. B. Nielson, and A. J. Holder. GAUSSVIEW User Manual. Gaussian: Pittsburgh, **2000**.
21. F. Odame, E. C. Hosten, and Z. R. Tshentu. *J. Struct. Chem.*, **2018**, *59*(8), 1804–1809.
22. F. Odame and E. C. Hosten. *Acta Chim. Slov.*, **2018**, *65*, 531–538.